Exotic phases of interacting p-band bosons

F. Hébert,[1] Zi Cai,[2,3] V. G. Rousseau,[4] Congjun Wu,[3] R. T. Scalettar,[5] and G. G. Batrouni[1,6]

[1]*INLN, Université de Nice-Sophia Antipolis, CNRS, 1361 route des Lucioles, 06560 Valbonne, France*

[2]*Physics Department, Arnold Sommerfeld Center for Theoretical Physics, and Center for NanoScience, Ludwig-Maximilians-Universität München, D-80333 München, Germany*

[3]*Department of Physics, University of California, San Diego, California 92093, USA*

[4]*Department of Physics and Astronomy, Louisiana State University, Baton Rouge, Louisiana 70803, USA*

[5]*Physics Department, University of California, Davis, California 95616, USA*

[6]*Institut Universitaire de France, 103 bd Saint Michel, 75005 Paris, France*

(Received 11 April 2013; published 17 June 2013)

We study a model of interacting bosons that occupy the first excited p-band states of a two-dimensional optical lattice. In contrast to the much studied single band Bose-Hubbard Hamiltonian, this more complex model allows for nontrivial superfluid phases associated with condensation at nonzero momentum and staggered order of the orbital angular momentum in addition to the superfluid-Mott insulator transition. More specifically, we observe staggered orbital angular momentum order in the Mott phase at commensurate filling and superfluidity at all densities. We also observe a transition between the staggered angular momentum superfluid phase and a striped superfluid, with an alternation of the phase of the superfluid along one direction. The transition between these two phases was observed in a recent experiment, which is then qualitatively well described by our model.

DOI: 10.1103/PhysRevB.87.224505 PACS number(s): 05.30.Jp, 03.75.Hh, 75.10.Jm, 03.75.Mn

I. INTRODUCTION

Superfluidity has attracted much attention since its discovery in bosonic ^{4}He and, later, in fermionic ^{3}He.[1] This phenomenon was studied in a wide range of systems ranging from excitons in quantum wells[2] to neutron stars.[3] Interest intensified following the experimental realization of confined ultracold atomic systems, in particular atomic Bose-Einstein condensates (BEC).[4–7] Many new possibilities become available when these systems are loaded in the lowest band of optical lattices where they are governed by the (bosonic or fermionic) Hubbard model with highly tunable parameters.[8] After their initial use to explore quantum phase transition between superfluid (SF) and Mott insulator (MI) phases[9] ultracold atomic gases have been used to study mixtures of particles[10,11] and, since then, more exotic pairing phenomena, including Fulde-Ferrell-Larkin-Ovchinnikov[12,13] or breached paired phases[14,15] in unbalanced fermionic systems, or to introduce the concept of countersuperfluidity in MI of boson mixtures.[16] Work on spinor condensates concentrated on the interplay between superfluid behavior and itinerant magnetism, especially through the study of spin-1 bosons.[17,18]

More recently, it was proposed to load the atoms in higher bands of the optical lattice in order to study further exotic forms of superfluidity.[19] In a three-dimensional cubic lattice there are three such states that are degenerate and correspond to the different states of orbital angular momentum $l = 1$ [$\mathbf{L}^2 = l(l+1) = 2$ in units of $\hbar^2$], whereas the unique ground state corresponds to $l = 0$. Due to the anisotropy used to produce two-dimensional square lattices, one of the orbitals has a larger energy than the other two. This reduces the model to only two species (the p_x and p_y states) in the low energy limit. On cubic or square lattices, the hopping parameters from a site to its neighbors are anisotropic and take two very different values depending on the hopping direction, parallel or perpendicular to the orbital axis. Isacsson and Girvin[19] studied the limit where the hopping in the transverse directions is totally suppressed. This led them to suggest that in two dimensions their model may develop a peculiar columnar phase ordering where the phases of particles in the $p_{x(y)}$ states are coherent along the $x(y)$ direction and uncorrelated in the transverse direction.

Bosons in high orbital bands are not in the true ground state. This feature gives rise to the possibility of new states of matter beyond the "no-node" theorem[20] that is obeyed by the conventional BECs of single component bosons. This theorem states that the many-body ground state wave functions of bosons under very general conditions are positive definite. It implies that time-reversal symmetry cannot be spontaneously broken. If the system has rotational symmetry, this theorem constrains the condensate wave functions to be rotationally invariant. In other words, conventional BECs are s-wavelike whose symmetry property is similar to s-wave superconductivity. Recently, unconventional symmetries have been introduced to the single-boson condensates in high orbital bands in optical lattices,[21,22] denoted as "unconventional BECs" (UBECs). Their condensate wave functions belong to nontrivial representations of the lattice point group. In other words, they are non-s-wave in analogy to unconventional pairing symmetries of superconductivity. Liu and Wu[22] studied analytically the UBECs in the p-orbital band with nonzero transverse hopping exhibiting a $p_x \pm ip_y$ type symmetry, and thus breaking time-reversal symmetry spontaneously with a complex-valued condensate wave function. They predicted for densities ρ larger than two particles per site, the existence of a superfluid phase where the system condenses at nonzero quasimomentum and which is accompanied by a staggered order of the orbital angular momentum (SAM). Recently, the model was studied using an effective action approach[23] and a similar SF phase with SAM order was predicted even for $\rho = 1$ as well as an antiferromagnetic Mott phase. Its physics was also examined in one dimension.[24] In solid state physics, phase-sensitive detections provide definitive evidence

for unconventional symmetries of the Cooper pair wave functions, such as the well known d-wave symmetry in high T_c cuprates.[25,26] In a corner junction experiment,[25] the d-wave symmetry generates an additional π flux in addition to fluxes from external magnetic fields, which modifies the observed Josephson currents in the junction. For the non-s-wave UBECs, phase-sensitive detection on condensate symmetries has also been proposed through Raman transition.[27]

Such an exotic SF phase was observed in a recent experiment by Wirth, Ölschläger, and Hemmerich[28–30] in a two-dimensional checkerboard lattice composed of s- and p-orbital sites and had been investigated theoretically by Cai *et al.*[31] The nearest neighbors of s sites being p sites, an atom cannot go directly from a p site to another as was the case in Liu and Wu's model.[21,22] However, the s sites do not introduce phase differences and thus only play the role of a neutral relay between p sites. Introducing a small anisotropy between the x and y axes, a transition between the condensed state at nonzero momentum and a striped phase where there is a phase alternation between different stripes was observed. BECs with unconventional condensate symmetries have also been observed in the solid state exciton-polariton lattice systems.[32]

In this work we will study the model originally proposed by Liu and Wu[22] with quantum Monte Carlo simulations. To reproduce qualitatively the different phases observed in Hemmerich's group experiment, we will add to the original model an anisotropy term in the form of an energy difference between p_x and p_y orbitals. We will use a simplified model that does not include the s sites present in the experiment, and hence is not able to reproduce the experimental results quantitatively. A complete model, including all p and s bands, was presented very recently by Ölschläger *et al.*[30] but is beyond the reach of our simulation tools. Finally, in addition to studying the superfluid phase, we will also focus on the insulating phases that arise in such systems for strong enough interactions and integer densities. In Sec. II of this article we will introduce and discuss the model. In Sec. III we will show that it can be mapped on a bosonic spin-1/2 model and establish the correspondence between the phases observed. In Sec. IV we will present the results of our simulations and conclude in Sec. V.

II. THE p-ORBITAL MODEL

We will study the model introduced in Refs. 21 and 22 for the two-dimensional square lattice and two-species ("spin-1/2") case. The system is then governed by the Hamiltonian

$$\begin{aligned} H = &+t_\parallel \sum_{\mathbf{r}} (p^\dagger_{x,\mathbf{r}} p_{x,\mathbf{r}+\hat{x}} + p^\dagger_{y,\mathbf{r}} p_{y,\mathbf{r}+\hat{y}} + \text{H.c.}) \\ &- t_\perp \sum_{\mathbf{r}} (p^\dagger_{x,\mathbf{r}} p_{x,\mathbf{r}+\hat{y}} + p^\dagger_{y,\mathbf{r}} p_{y,\mathbf{r}+\hat{x}} + \text{H.c.}) \\ &+ \frac{U}{2} \sum_{\mathbf{r}} \left(n^2_{\mathbf{r}} - \frac{L^2_{z,\mathbf{r}}}{3} \right) + \Delta \sum_{\mathbf{r}} (n_{x,\mathbf{r}} - n_{y,\mathbf{r}}), \end{aligned} \quad (1)$$

where $p_{x(y),\mathbf{r}}$ is the destruction operator of a particle located on site $\mathbf{r} = (r_x, r_y)$ of an $L \times L$ square lattice in the $p_x(p_y)$ state; and $\hat{x}$ and $\hat{y}$ are the primitive vectors of the square lattice. The number operators are $n_{x(y),\mathbf{r}} = p^\dagger_{x(y),\mathbf{r}} p_{x(y),\mathbf{r}}$ and $n_{\mathbf{r}} = n_{x,\mathbf{r}} + n_{y,\mathbf{r}}$; and L_z is the on-site orbital angular momentum operator defined as

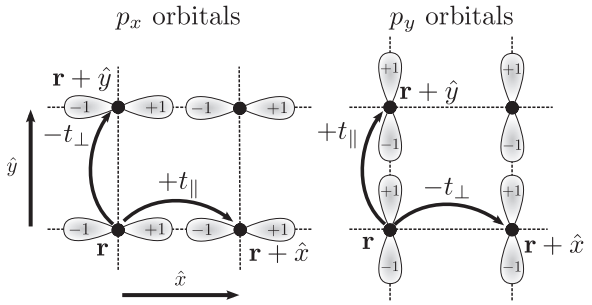

FIG. 1. Hopping parameters on the square lattice for p_x and p_y orbitals. Because $p_{x,(y)}$ orbitals are parity odd, the overlap of orbitals changes sign depending on the direction. Along the parallel direction (x for p_x orbitals, y for p_y orbitals), the overlap is negative, which gives a positive $+t_\parallel$ hopping parameter. On the other hand, along the perpendicular direction, there is a conventional negative hopping parameter $-t_\perp$.

$$L_{z,\mathbf{r}} = -i(p^\dagger_{x,\mathbf{r}} p_{y,\mathbf{r}} - p^\dagger_{y,\mathbf{r}} p_{x,\mathbf{r}}). \quad (2)$$

We remark that $L^2_{z,\mathbf{r}}$ is not diagonal in this basis and contains terms that transform two particles of one species into two particles of the other species.

Since the overlap of p orbitals on neighboring sites is different in the directions parallel or perpendicular to their spatial orientation, there are two different hopping parameters. $t_\perp$ is typically smaller than $t_\parallel$ (Fig. 1). Moreover, due to the phase difference between the two parts of the p orbitals, the two hopping terms have different signs [Eq. (1)], being positive in the parallel direction ($+t_\parallel$), whereas the perpendicular hopping term maintains the conventional negative sign ($-t_\perp$). We will concentrate on the case where $t_\perp = t_\parallel = t$, but also retain the sign difference which is qualitatively the most important characteristic of this model. The parameter t sets the energy scale. The interaction part of the Hamiltonian [Eq. (1)] includes a conventional on-site repulsion (the $n^2_{\mathbf{r}}$ term) and a term that maximizes the on-site angular momentum (the $L^2_{z,\mathbf{r}}$ term). This is essentially the physics of second Hund's rule applied to the bosonic orbital system: Complex orbitals are spatially more extended to save repulsive interactions. The last term in the Hamiltonian [Eq. (1)] corresponds to a tunable difference in energy Δ between the p_x and p_y orbitals, due to a corresponding anisotropy in the lattice.

In the noninteracting limit, the energy dispersion for p_x particles[22] takes the form $\epsilon_x(\mathbf{k}) = 2t[\cos(k_x) - \cos(k_y)]$, where $\mathbf{k} = (k_x, k_y)$, $k_{x(y)} = 2\pi K_{x(y)}/L$, and $K_{x(y)}$ is an integer. For p_y particles $\epsilon_y(\mathbf{k}) = -\epsilon_x(\mathbf{k})$. Since the energy minima appear at $\mathbf{k} = (\pi, 0)$ for the p_x particles and at $\mathbf{k} = (0, \pi)$ for the p_y particles, it is expected for the system to condense at nonzero momentum.

In the interacting case, the interaction energy is minimized by maximizing $L^2_{z,\mathbf{r}}$ on a given site, that is by putting all the particles in the same state corresponding to either $L_z = +1$ or $L_z = -1$: $|L_z = +1\rangle \propto |p_x\rangle + i|p_y\rangle$ and $|L_z = -1\rangle \propto |p_x\rangle - i|p_y\rangle$. With these on-site states, it is then possible to

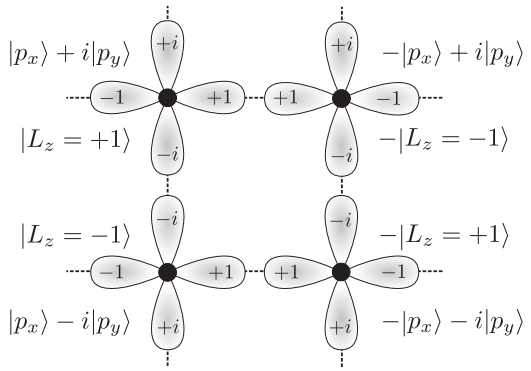

FIG. 2. Staggered orbital angular momentum order. A configuration having states proportional to $|L_z = \pm 1\rangle$ on each site maximizes L_z^2, minimizing the interaction energy. Concentrating on the p_x orbital, there is a phase alternation along the x direction and a phase coherence along the y direction, which minimizes the kinetic energy and corresponds to the condensation with wave vector $\mathbf{k} = (\pi,0)$. The same phenomenon is observed for the p_y orbitals, with reversed axes and $\mathbf{k} = (0,\pi)$. This gives an alternation of sites with $L_z = \pm 1$ and thus a staggered order for the angular momentum along z.

minimize the hopping energy by using a configuration[22] that gives a phase difference along the longitudinal hopping and a phase match for transverse hopping. Such a configuration is represented in Fig. 2; it exhibits a checkerboard pattern of $L_z = \pm 1$ sites. This is the staggered angular momentum order mentioned in the Introduction, and it is clear that it is compatible with a phase ordering that corresponds to the condensation at nonzero momentum for both p_x and p_y particles.

Finally the Δ term in Eq. (1) should suppress this kind of order since it requires having the same number of p_x and p_y particles by increasing the density of p_y particles. If the system remains superfluid when it is composed mostly of p_y particles, the phase will alternate between sites along the y direction and will be coherent in the x direction, thus forming stripes along the x axis. We will call this phase a striped superfluid (see Fig. 3).

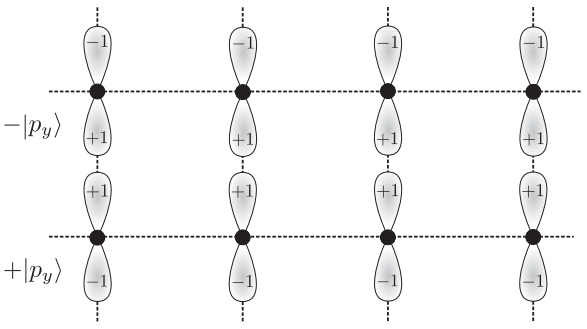

FIG. 3. Stripe phase. Due to the different signs of the hopping parameters, when the system is composed of just one species (p_y in this figure), it will have phase alternation along the parallel (y) direction and phase coherence along the transverse (x) direction to minimize the kinetic energy. This forms stripes aligned with the transverse direction and striped superfluid phases can be observed.

III. MAPPING ON A SPIN-1/2 MODEL

The positive parallel hopping term in Eq. (1) generates a sign problem for quantum Monte Carlo simulations. (In this work we use the stochastic Green function algorithm.[33,34]) However, the Hamiltonian can be mapped onto a spin-1/2 model free of this problem.[35,36] We define the spin-1/2 bosonic operators

$$b_{\uparrow,\mathbf{r}} = i(-1)^x p_{x,\mathbf{r}}, \quad b_{\downarrow,\mathbf{r}} = (-1)^y p_{y,\mathbf{r}}. \tag{3}$$

This transformation gives a direct equivalence between densities of $\uparrow$ ($\downarrow$) and $p_x(p_y)$ particles. Then the corresponding spin-1/2 operators are defined:[37] $S_{z,\mathbf{r}} = (n_{\uparrow,\mathbf{r}} - n_{\downarrow,\mathbf{r}})/2$, $S_{+,\mathbf{r}} = b^\dagger_{\uparrow,\mathbf{r}} b_{\downarrow,\mathbf{r}}$, and $S_{-,\mathbf{r}} = b^\dagger_{\downarrow,\mathbf{r}} b_{\uparrow,\mathbf{r}}$. With these definitions the model is rewritten, up to some constants, as

$$H_{1/2} = -t \sum_{\mathbf{r}} \sum_{\hat{\alpha}=\hat{x},\hat{y}} \sum_{\sigma=\uparrow,\downarrow} (b^\dagger_{\sigma,\mathbf{r}} b_{\sigma,\mathbf{r}+\hat{\alpha}} + \text{H.c.}) + \sum_{\mathbf{r}} \left(U \frac{n_{\mathbf{r}}(n_{\mathbf{r}}-1)}{2} - \frac{2U}{3} S^2_{x,\mathbf{r}} + 2\Delta S_{z,\mathbf{r}} \right), \tag{4}$$

where $S_{x,\mathbf{r}} = (S_{+,\mathbf{r}} + S_{-,\mathbf{r}})/2$ and plays a role similar to the $L_{z,\mathbf{r}}$ operator in the original model. This model is free of the sign problem as all the hopping terms and the on-site nondiagonal term are negative.

Up to the external field term along the z direction, this is the model that was studied in Refs. 35 and 36 with $U_0 = U$ and $U_2 = -U/3$ for the values of the parameters used in these articles. For $\Delta = 0$, it was shown that the system is always ferromagnetic at low temperature. On a given site, the absolute value of the projection of the spin along the x axis is maximized due to the negative $S^2_{x,\mathbf{r}}$ term. The hopping of the particles then creates an effective ferromagnetic coupling between spins located on different sites. This ferromagnetic order is of the Ising class because of the anisotropy introduced by the $S^2_{x,\mathbf{r}}$ term. It is measured by calculating the spin-spin correlation function along the x axis, related to the correlation of angular momenta $C_z(\mathbf{R})$ in the original model [$\mathbf{R} = (R_x, R_y)$],

$$C_z(\mathbf{R}) = \langle L_{z,\mathbf{r}} L_{z,\mathbf{r}+\mathbf{R}} \rangle = 4(-1)^{R_x+R_y} \langle S_{x,\mathbf{r}} S_{x,\mathbf{r}+\mathbf{R}} \rangle. \tag{5}$$

That is, the observed ferromagnetism in the spin-1/2 model corresponds to the staggered angular momentum predicted in the p-band model.

Although it always adopts ferromagnetic behavior at $\Delta = 0$, the system can be in different incompressible Mott phases at integer densities and large enough interaction U, or in a superfluid phase for noninteger densities and for integer densities at low enough interaction U. A constant value, at long distance, of the one particle Green functions $G_\sigma(\mathbf{R}) = \langle b_{\sigma,\mathbf{r}} b^\dagger_{\sigma,\mathbf{r}+\mathbf{R}} \rangle$ shows that the particles have condensed and that the system is superfluid. In terms of p-band particles, the Green functions $G_{x(y)}(\mathbf{R}) = \langle p_{x(y),\mathbf{r}} p^\dagger_{x(y),\mathbf{r}+\mathbf{R}} \rangle$ have the following expressions:

$$G_x(\mathbf{R}) = (-1)^{R_x} G_\uparrow(\mathbf{R}), \quad G_y(\mathbf{R}) = (-1)^{R_y} G_\downarrow(\mathbf{R}). \tag{6}$$

That is, a superfluid/BEC phase for spin-1/2 particles translates directly into the BEC at nonzero momentum phase for the p-band particles, because of the real space phase factors $(-1)^{R_x}$ and $(-1)^{R_y}$.

The same correspondence holds for the Fourier transforms of these functions, namely the spin-1/2 magnetic structure factor at $\mathbf{k} = (0,0)$ becoming an angular momentum structure factor at $\mathbf{k} = (\pi,\pi)$. We will call this quantity S_{SAM} in the following, where

$$S_{\mathrm{SAM}} = \frac{1}{L^2}\sum_{\mathbf{R}}(-1)^{R_x+R_y}C_z(\mathbf{R}). \tag{7}$$

The density of condensed spin-1/2 particles at $\mathbf{k} = (0,0)$ becomes the density of condensed p_x and p_y particles at $\mathbf{k} = (\pi,0)$ and $\mathbf{k} = (0,\pi)$, respectively, which will be denoted ρ_{cx} and ρ_{cy} in the following, where

$$\rho_{cx(y)} = \frac{1}{L^2}\sum_{\mathbf{R}}(-1)^{R_{x(y)}}G_{x(y)}(\mathbf{R}). \tag{8}$$

Finally, in the spin-1/2 model, it is possible to measure the superfluid density ρ_s through the fluctuations of total winding numbers[38]

$$\rho_s = \frac{\langle W_x^2 + W_y^2\rangle}{4\beta t}. \tag{9}$$

At zero temperature, the superfluid density ρ_s and the condensed densities ρ_{cx} and ρ_{cy} are generally nonzero simultaneously so we will use ρ_s to determine if we are in the condensed phase for both models.

IV. SIMULATION RESULTS

Quantum Monte Carlo simulations using the SGF algorithm[33,34] allow us to study the spin-1/2 model at finite temperature for $L \times L$ lattices up to $L = 10$ and inverse temperature up to $\beta t = 80$. The difficulty of the simulations is caused by the S_x^2 interaction term which changes the spin projection of the particles. The simulations are performed at low temperatures in order to obtain the behavior of the ground states. We will concentrate on $\Delta \neq 0$.

A. Phase diagrams

We expect Mott phases to appear for large enough interactions and integer densities ρ. To determine the extent of these phases in the $(t/U,\mu/U)$ plane for a given value of Δ we calculate the energy $E(N)$ at low temperature for $N = \rho L^2$, $N+1$, and $N-1$ particles. We then determine the boundaries of the Mott lobe as $\mu_+ = E(N+1) - E(N)$ and $\mu_- = E(N) - E(N-1)$, and μ_+ is larger than μ_- by a finite value, the charge gap. As expected, we find Mott phases occur for integer densities $\rho = 1$ and $\rho = 2$. (We did not go beyond $\rho = 2$.) We observe that the boundaries of the different phases are not changed much when Δ is varied (Fig. 4). Since the energy is a local quantity which is not very sensitive to system size, the boundaries of the Mott lobes are little changed with system size as seen in Fig. 5. We will detail below the nature of these three phases for different densities.

B. $\rho = 1$ case

In Fig. 6 we present the dependence of the particles, superfluid, and condensate densities and the angular momentum structure factor on the interaction U at fixed density $\rho = 1$

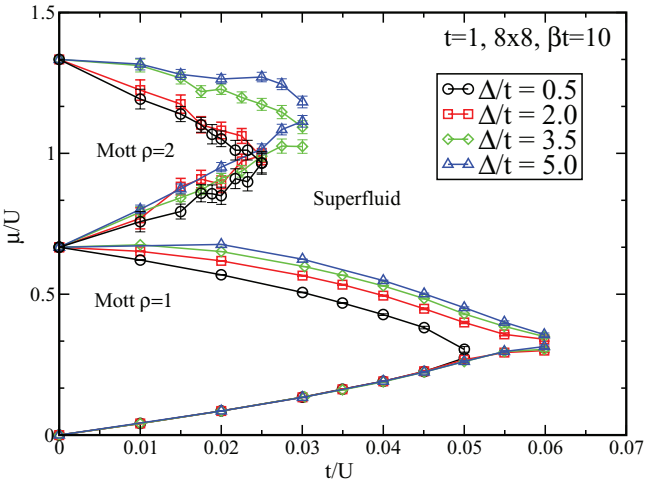

FIG. 4. (Color online) Phase diagram for $\Delta/t = 0.5$, 2.0, 3.5, and 5.0. We observe two Mott phases and a superfluid phase. The extents of the Mott phases are not varying a lot with Δ, especially for the $\rho = 1$ Mott phase and large values of Δ.

and $\Delta = 0.5$. We observe, as expected for nonzero Δ, that ρ_y is larger than ρ_x. As U is increased, ρ_x, ρ_y, and S_{SAM} show a nonmonotonic behavior. There is a correlation between ρ_x and S_{SAM} which can be understood by noting that S_{SAM} order requires a superposition of p_x and p_y particles that is possible only when ρ_x is not zero. However, the superfluid density decreases monotonically with U and the system is driven into an incompressible Mott phase where double occupancy is suppressed at large U. In this Mott phase the model can then be mapped onto an effective anisotropic spin-1/2 Heisenberg model. For $\Delta = 0$, the larger coupling of the Heisenberg model is along the x axis and is equal to $J_x = -9t^2/U$ which leads to ferromagnetic order. This is SAM order in terms of p-band bosons.[16,39] The Δ term acts as an external magnetic field along the z axis and tends to destroy the ferromagnetic/SAM order. In Fig. 6 the Mott phase is composed only of p_y particles ($\rho_y \simeq 1$) as Δ is large enough to overcome the ordering of effective spins along the x axis. There is, then, no SAM order

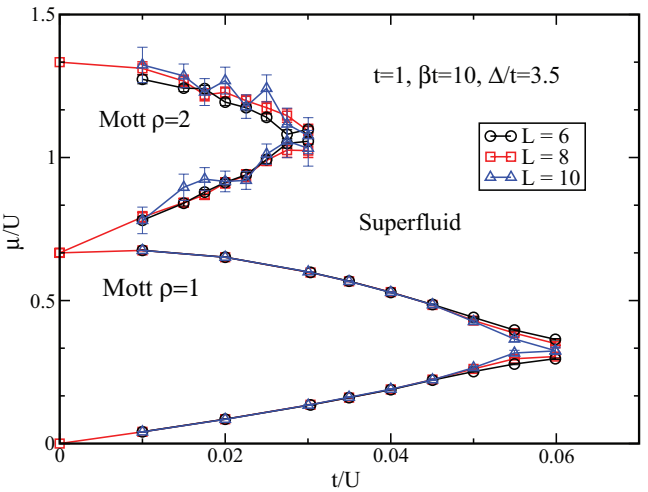

FIG. 5. (Color online) Phase diagram for $\Delta/t = 3.5$ and different sizes. The finite size effects are negligible.

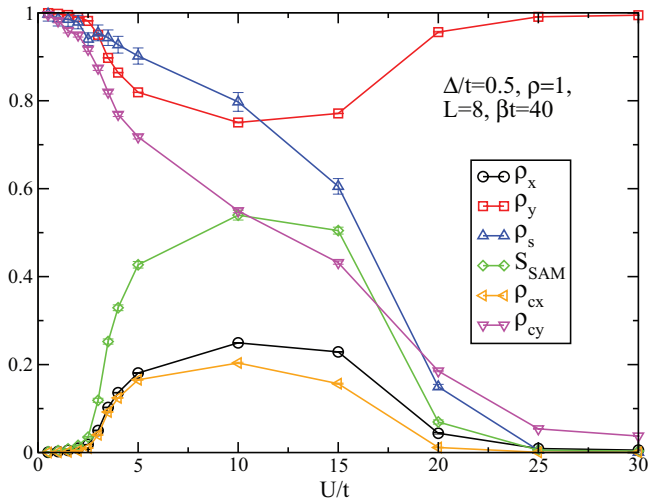

FIG. 6. (Color online) Cut in the phase diagram at $\rho = 1$ and $\Delta = 0.5$. The system goes from a Bose condensed phase at low interaction to a Mott phase as ρ_s goes to zero with increasing interaction U. There is an intermediate SAM-Bose condensed phase.

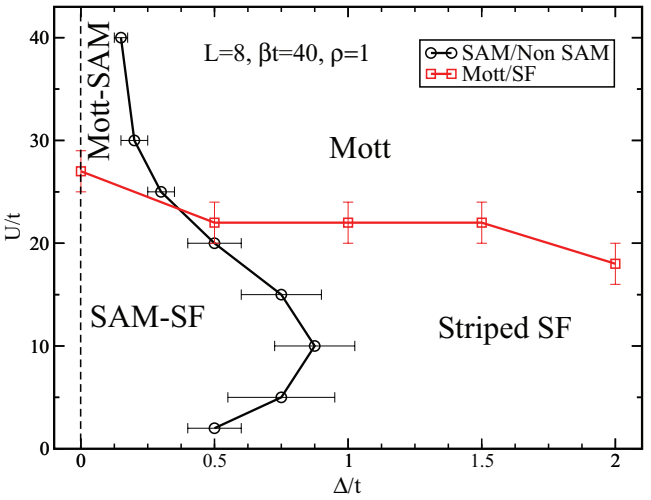

FIG. 8. (Color online) Phase diagram for $\rho = 1$ as a function of U/t and Δ/t. There are four different phases: a Mott phase, a Mott phase with staggered orbital momentum (SAM) order, a superfluid phase with SAM order, and a striped superfluid.

in the Mott phase in this case. However, the Mott phase shows a SAM order for small enough values of Δ (see Fig. 7, bottom). In the Mott phase there is then a competition between the weak effective coupling of the moments and the anisotropy term. As U become large, the effective coupling decreases as $1/U$ and the system always ends up in a Mott phase composed only of p_y particles. However, for low enough values of Δ, there exists a SAM Mott region.

Returning to the low interaction regime, there are two different superfluid phases observed in Fig. 6. At low interaction U, the system is well described as a collection of free particles and, since the Δ term lowers the energy of p_y states, the particles condense in this state. L_z is then on average zero on each site and no SAM is observed. The p_y bosons form a condensate and the phase is a striped superfluid because ρ_{cy} is nonzero. For intermediate interaction, we observe a SAM superfluid where ρ_{cx}, ρ_{cy}, and S_{SAM} are nonzero at the same time. For such moderate U, the interaction is not large enough to block particles in a Mott phase. To lower the interaction energy, the system adopts states that have the largest possible absolute value of $L_{z,\mathbf{r}}$ on a site and the hopping terms lock the relative phases into an SAM order. One should notice however, that when there is only one particle on a site, the value of $L^2_{z,\mathbf{r}}$ is fixed to one whatever the state of the particle and that the minimization of the interaction energy takes place only when there are fluctuations of the number of particles. As in the Mott

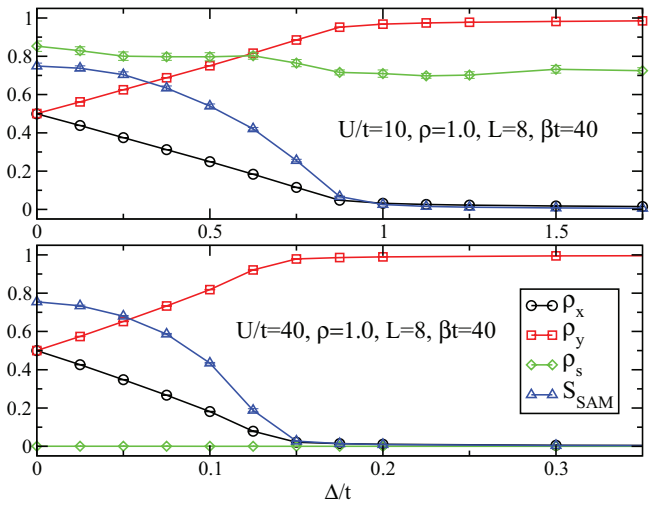

FIG. 7. (Color online) Cuts in the phase diagram at $\rho = 1$ as a function of Δ/t. At $U/t = 10$ (top), the system is always in the superfluid phase ($\rho_s \neq 0$) and we observe a staggered angular momentum order when $\Delta < 1$. For $\Delta > 1$, the superfluid is composed of only one dominant species. The same happens in the Mott phase for large interaction $U/t = 40$ (bottom) with a smaller value ($\Delta \simeq 0.15$) for the disappearance of the SAM order.

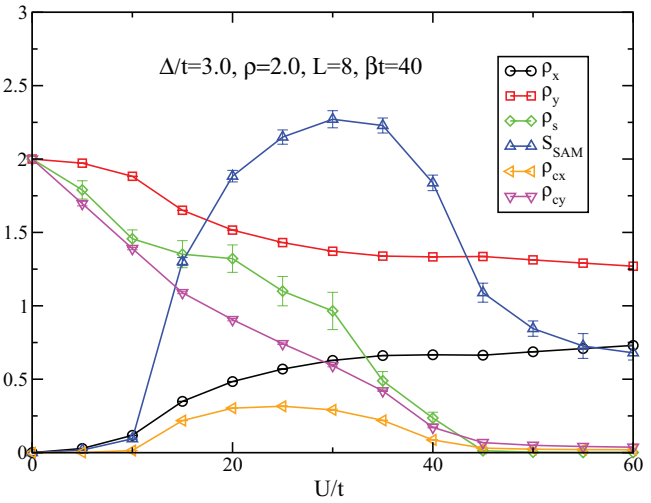

FIG. 9. (Color online) Cut in the phase diagram at $\rho = 2$ as a function of U/t, the quantities and the observed behavior are similar to the $\rho = 1$ case (see Fig. 6) but the S_{SAM} order is more robust as it is still nonzero in the Mott phase, despite the much larger value of Δ ($\Delta/t = 3$ in this case compared to $\Delta/t = 0.5$ in Fig. 6).

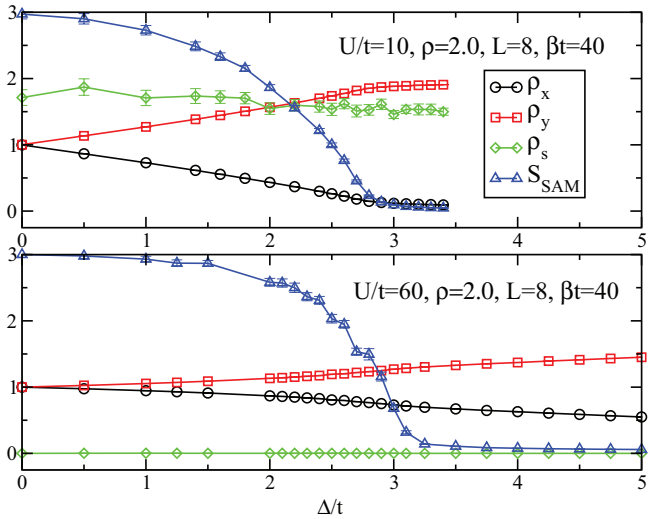

FIG. 10. (Color online) Cut in the phase diagram at $\rho = 2$ as a function of Δ/t. The quantities and the observed behavior are similar to the $\rho = 1$ case (see Fig. 7) with a more robust SAM order persisting up to $\Delta/t \simeq 3$.

case, the SAM order will disappear if the system is composed of only p_y particles due to a large value of Δ (see Fig. 7, top).

Finally, using different cuts in the phase diagram at fixed Δ or U, similar to Figs. 6 and 7, we map the phase diagram presented in Fig. 8 for $\rho = 1$. We observe that for the range of values we studied, the SAM order completely disappears for $\Delta > 1$ and the system is in a Mott phase for $U > 25$.

C. $\rho = 2$ case

We performed the same analysis for the $\rho = 2$ case and found similar results (see Figs. 9, 10, and 11). However, the SAM is much more robust, as it persists up to $\Delta = 4$. This can be understood by recalling that the $L_{z\mathbf{r}}^2$ term scales as the square of the density and that, for $\rho > 1$, the interaction energy

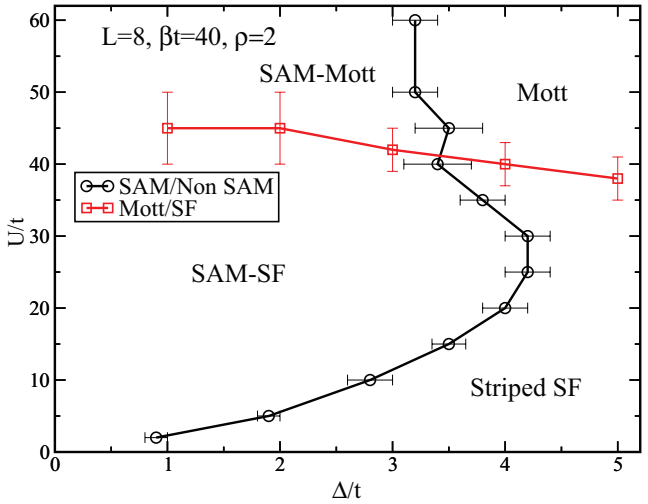

FIG. 11. (Color online) Phase diagram for $\rho = 2$ as a function of U/t and Δ/t. The SAM phases are more robust than in the $\rho = 1$ case (Fig. 8) but the same four phases are observed.

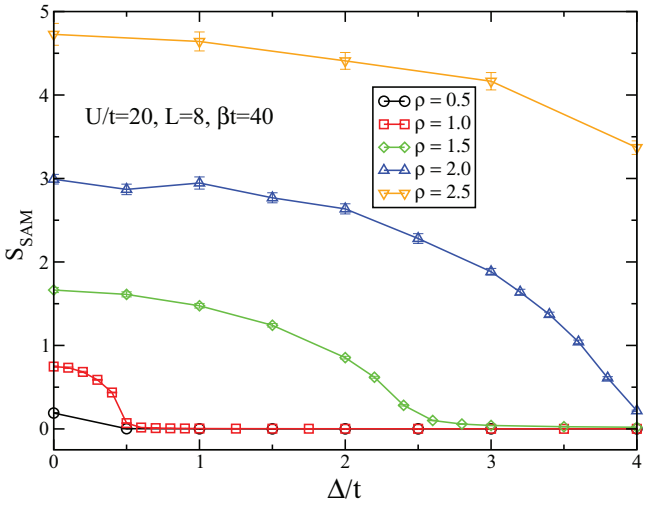

FIG. 12. (Color online) Cuts as functions of Δ for $U = 20$ and different integer and noninteger densities. For these regimes, the system is always superfluid, even for integer densities. We observe that, as the density is increased, the structure factor S_{SAM} becomes larger and larger and persists for larger values of Δ. The SAM order is found for all densities, provided Δ is small enough.

term favors the development of local moments with $|L_{z,\mathbf{r}}| > 1$. Thus the associated SAM coupling of the angular momentum should grow rapidly with the density and the stripe phase is therefore more difficult to observe.

D. Noninteger densities

At noninteger densities the system is of course always superfluid. As at commensurate fillings $\rho = 1$ and $\rho = 2$, we observe a transition between the SAM superfluid phase and the stripe superfluid as Δ is increased. The limiting value of Δ grows with increasing density, a trend already evident in comparing results for the two integer fillings (Fig. 12). The value of Δ at which the SAM disappears corresponds to the system being populated almost entirely by p_y particles. We observe the SAM order for any density, which complements the results from Ref. 21 that concentrated mostly on the $\rho \geqslant 2$ cases.

V. CONCLUSION

We studied a model for p-band superfluidity[21,22] using exact quantum Monte Carlo simulations. We found that the phase diagram of the model is composed of a striped superfluid, a superfluid with simultaneous staggered angular momentum order (SAM), a SAM Mott, and a Mott phase. Our QMC simulations indicate that the SAM superfluid phase can be observed for any density, although it becomes more robust as the density is increased. The presence of the SAM order in the $\rho = 1$ Mott can be understood with an analysis in terms of an effective Heisenberg model. The larger density cases were extensively studied analytically in Refs. 21 and 22.

Despite its differences with the experiment of Hemmerich and co-workers (namely the absence of the s-wave sites), the simple model studied here gives a good qualitative description of the results. It reproduces the two observed

superfluid phases, the SAM and stripe superfluids, with the same condensations at nonzero momenta. It also reproduces the transition between these two exotic superfluids driven by the energy difference Δ between the two species. Moreover, our results suggest that in a system with stronger repulsive interaction, a similar phase transition between a SAM and a non-SAM phase could be observed in a Mott insulating phase.

Here we focused exclusively on the isotropic case $t_\perp = t_\parallel$, although an experimental realization would have anisotropies $t_\perp \neq t_\parallel$. We have done some preliminary simulations (not shown here) for $t_\perp$ and $t_\parallel$ values that are not very different. These indicate that the physics remains qualitatively the same. The case of extreme anisotropy $t_\perp/t_\parallel \ll 1$ and even $t_\perp = 0$ does differ[19] and merits special attention.

ACKNOWLEDGMENTS

We would like to thank L. de Forge de Parny for stimulating discussions. This work was supported by the CNRS-UC Davis EPOCAL LIA joint research grant; by NSF Grant OISE-0952300; and ARO Award W911NF0710576 with funds from the DARPA OLE Program. C.W. is supported by NSF DMR-1105945 and AFOSR FA9550-11-1-0067(YIP).

[1] D. R. Tilley and J. Tilley, *Superfluidity and Superconductivity* (Institute of Physics, Bristol, 1990).
[2] S. A. Moskalenko, Fiz. Tverd. Tela **4**, 276 (1962); C. Comte and P. Noziéres, J. Phys. **43**, 1069 (1982).
[3] A. B. Migdal, Nucl. Phys. **13**, 655 (1959).
[4] M. R. Matthews, B. P. Anderson, P. C. Haljan, D. S. Hall, C. E. Wieman, and E. A. Cornell, Phys. Rev. Lett. **83**, 2498 (1999).
[5] R. Onofrio, C. Raman, J. M. Vogels, J. R. Abo-Shaeer, A. P. Chikkatur, and W. Ketterle, Phys. Rev. Lett. **85**, 2228 (2000).
[6] F. Dalfovo, S. Giorgini, L. P. Pitaevskii, and S. Stringari, Rev. Mod. Phys. **71**, 463 (1999).
[7] A. J. Leggett, Rev. Mod. Phys. **73**, 307 (2001).
[8] D. Jaksch, C. Bruder, J. I. Cirac, C. W. Gardiner, and P. Zoller, Phys. Rev. Lett. **81**, 3108 (1998).
[9] M. Greiner, O. Mandel, T. Esslinger, T. W. Hänsch, and I. Bloch, Nature (London) **415**, 39 (2002).
[10] M. W. Zwierlein, A. Schirotzek, C. H. Schunck, and W. Ketterle, Science **311**, 492 (2006).
[11] Y-A. Liao, A-S. C. Rittner, T. Paprotta, W. Li, G. B. Partridge, R. G. Hulet, S. K. Baur, and E. J. Mueller, Nature (London) **467**, 567 (2010).
[12] P. Fulde and R. A. Ferrell, Phys. Rev. **135**, 550 (1964).
[13] A. I. Larkin and Yu. N. Ovchinnikov, Sov. Phys. JETP **20**, 762 (1965).
[14] G. Sarma, J. Phys. Chem. Solids **24**, 1029 (1963).
[15] W. V. Liu and F. Wilczek, Phys. Rev. Lett. **90**, 047002 (2003).
[16] A. B. Kuklov and B. V. Svistunov, Phys. Rev. Lett. **90**, 100401 (2003).
[17] Y. Kawaguchi and M. Ueda, Phys. Rep. **520**, 253 (2012).
[18] D. M. Stamper-Kurn and W. Ketterle, in *Coherent Atomic Matter Waves*, Les Houches Summer School Session LXXII (Springer, Berlin, 2001), pp. 137–217.
[19] A. Isacsson and S. M. Girvin, Phys. Rev. A **72**, 053604 (2005).
[20] R. P. Feynman, *Statistical Mechanics* (Perseus Books, Reading, MA, 1998).
[21] C. Wu, Mod. Phys. Lett. B **23**, 1 (2009).
[22] W. V. Liu and C. Wu, Phys. Rev. A **74**, 013607 (2006).
[23] X. Li, E. Zhao, and W. V. Liu, Phys. Rev. A **83**, 063626 (2011).
[24] X. Li, Z. Zhang, and W. V. Liu, Phys. Rev. Lett. **108**, 175302 (2012).
[25] D. A. Wollman, D. J. Van Harlingen, W. C. Lee, D. M. Ginsberg, and A. J. Leggett, Phys. Rev. Lett. **71**, 2134 (1993).
[26] C. C. Tsuei, J. R. Kirtley, C. C. Chi, L. S. Yu-Jahnes, A. Gupta, T. Shaw, J. Z. Sun, and M. B. Ketchen, Phys. Rev. Lett. **73**, 593 (1994).
[27] Z. Cai, L. M. Duan, and C. Wu, Phys. Rev. A **86**, 051601(R) (2012).
[28] G. Wirth, M. Ölschläger, and A. Hemmerich, Nat. Phys. **7**, 147 (2011).
[29] M. Ölschläger, G. Wirth, T. Kock, and A. Hemmerich, Phys. Rev. Lett. **108**, 075302 (2012).
[30] M. Ölschläger, T. Kock, G. Wirth, A. Ewerbeck, C. Morais Smith, and A. Hemmerich, arXiv:1305.1177.
[31] Z. Cai and C. Wu, Phys. Rev. A **84**, 033635 (2011).
[32] N. Y. Kim, K. Kusudo, C. Wu, N. Masumoto, A. Löffler, S. Höfling, N. Kumada, L. Worschech, A. Forchel, and Y. Yamamoto, Nat. Phys. **7**, 681 (2011).
[33] V. G. Rousseau, Phys. Rev. E **77**, 056705 (2008).
[34] V. G. Rousseau, Phys. Rev. E **78**, 056707 (2008).
[35] L. De Forges De Parny, F. Hébert, V. G. Rousseau, and G. G. Batrouni, Eur. Phys. J. B **85**, 169 (2012).
[36] L. De Forges De Parny, F. Hébert, V. G. Rousseau, R. T. Scalettar, and G. G. Batrouni, Phys. Rev. B **84**, 064529 (2011).
[37] A. Auerbach and D. P. Arovas, in *Introduction to Frustrated Magnetism* Springer Series in Solid-State Sciences Vol. 164 (Springer, Berlin, 2011), p. 365.
[38] E. L. Pollock and D. M. Ceperley, Phys. Rev. B **36**, 8343 (1987).
[39] M. Foss-Feig and A. M. Rey, Phys. Rev. A **84**, 053619 (2011).